Original Article
J Vet Sci 2017, 18(4), 507-514 · https://doi.org/10.4142/jvs.2017.18.4.507

Quantitative evaluation of renal parenchymal perfusion using contrast-enhanced ultrasonography in renal ischemia-reperfusion injury in dogs

Gahyun Lee, Sunghoon Jeon, Sang-kwon Lee, Byunggyu Cheon, Sohyeon Moon, Jun-Gyu Park, Kyoung-Oh Cho, Jihye Choi*

College of Veterinary Medicine, Chonnam National University, Gwangju 61186, Korea

This study evaluated whether renal perfusion changes can be noninvasively estimated by using contrast-enhanced ultrasonography (CEUS) in renal ischemia-reperfusion injury and investigated the correlation between renal perfusion measured by CEUS and necrosis and apoptosis of renal tubular epithelial cells. In six dogs with experimentally induced renal ischemia-reperfusion injury, changes in time to peak intensity, peak intensity, and area under the curve were measured on CEUS. Peak intensity and area under the curve of the renal cortex began to decrease on day 1 (about 20% lower than baseline) and reached the lowest levels (about 50% of baseline) on day 4. They then gradually increased until day 10, at which time peak intensity was about 87% and area under the curve was about 95% of baseline; neither fully recovered. Both parameters were strongly correlated with the necrosis scores on histopathologic examination on day 4 ($r = -0.810$ of peak intensity and $r = -0.886$ of area under the curve). CEUS allowed quantitative evaluation of perfusion changes in acute renal ischemia-reperfusion injury, and CEUS results were correlated with renal tubular damage on histopathologic examination. Thus, CEUS could be a noninvasive, quantitative diagnostic method for determining progress of renal ischemia-reperfusion injury.

Keywords: contrast-enhanced ultrasonography, dogs, renal tubular damage, reperfusion injury, time-intensity curve

Introduction

Acute renal tubular necrosis resulting from ischemia-reperfusion injury (IRI) is one of the most common causes of renal dysfunction and delayed graft function after renal transplantation and develops in 2%–4% of transplants from living related donors and 5%–20% of renal allografts from human cadavers [1,2,9]. IRI begins with adenosine triphosphate depletion in tissues and cells during the ischemic phase, followed by oxidative damage during the reperfusion phase [1,20,28]. In the latter phase, the expressions of biomarker proteins such as kidney injury molecule-1 and clusterin increase [16,24]. IRI induces renal vascular and interstitial damage and leads to vascular endothelial remodeling and changes in renal perfusion such as alteration of capillary and tubular flow and water content [23,27]. Necrosis and apoptosis of renal tubular epithelial cells, interstitial fibrosis, and eventually renal atrophy can develop. In such a process, aggregate damaged tissue can cause renal cell death, renal failure, delayed graft function, and renal graft rejection [22,26].

There is a need for more precise and sensitive markers to monitor acute tubular necrosis, even though urinalysis, serum blood urea nitrogen (BUN) and creatinine analysis, and ultrasonography can be used. A needle core biopsy is required for histopathological assessment with an associated risk of additional renal damage, perirenal hematoma, bleeding injury to the adjacent viscera, and graft loss [4,18,29].

The accurate measurement of renal perfusion in the early period of IRI can provide important clinical insight into renal function and mortality in acute renal tubular injury [14,17]. Doppler ultrasonography has limited efficacy in assessing renal perfusion because it has low sensitivity for slow blood flow, is angle dependent, and can only assess intravascular blood flow, not microcirculation [6,26].

The use of a contrast agent improves the sensitivity of ultrasonography for detecting vascularization with low blood velocity and a small volume within the parenchyma [8,21]. Microbubbles in the contrast agent do not leave the blood vessels, are not excreted by the kidney, and are not affected by glomerular filtration or tubular transport. Moreover, a

Received 24 Oct. 2016, Revised 9 Jan. 2017, Accepted 7 Feb. 2017
*Corresponding author: Tel: +82-62-530-2821; Fax: +82-62-530-2809; E-mail: imsono@chonnam.ac.kr
pISSN 1229-845X
eISSN 1976-555X

microbubble ultrasound contrast agent is not nephrotoxic as it is excreted through the lung, whereas an iodine contrast agent may be toxic as it is excreted via the kidney [31]. Therefore, contrast-enhanced ultrasonography (CEUS) has been used to depict altered renal perfusion in patients with focal renal ischemia, partially compensated shock, and poorly functioning renal transplants [12,27]. CEUS can quantitatively assess blood perfusion based on quantitative variables such as peak intensity and area under the curve (AUC), indicative of blood volume, and time to peak intensity, indicative of blood velocity [7].

This study was performed based on the hypotheses that CEUS can detect the renal parenchymal perfusion changes after renal IRI injury, and that the quantitative data estimated by CEUS may be reliable for renal damage and recovery assessment compared that derived from histopathologic results. Herein, perfusion changes of the renal cortex and medulla were quantitatively evaluated by using CEUS during the ischemic renal damage and recovery phases in a canine renal IRI model, and the correlation between CEUS results and necrosis and apoptosis within the renal tubules on histopathological examination was investigated.

Materials and Methods

The animals in this study were cared for in accordance with The Guide for Care and Use of Laboratory Animal Research Center, and all experiments were approved by the Institutional Animal Care and Use Committee at Chonnam National University (CNU IACUC-YB-R-2014-38).

Six 3-year-old intact male Beagle dogs weighing 8.5 to 12.5 kg (9.83 ± 1.19 kg) were used. A diagram of the schedule for the experimental procedures is presented in Fig. 1. Physical examination, systemic blood pressure, complete blood count, serum biochemistry, electrolytes, urine-specific gravity, urinary protein to creatinine ratio (UPC; Catalyst Dx Chemistry Analyzer; IDEXX Laboratories, USA), radiography, and ultrasonography were performed to collect baseline data.

Power Doppler and CEUS were performed by using the same instrument (ProSound Alpha 7; Hitachi-Aloka, Japan) with a 10 MHz linear transducer under anesthesia with intramuscular injections of zolazepam/tiletamine (Zoletil; Virbac, France) 1.5 mg/kg and medetomidine (Domitor; Orion, Finland) 0.03 mg/kg. Power Doppler ultrasonography was performed by using a 7.27 MHz Doppler frequency, a 1.2 kHz pulse repetition frequency, and a 3 cm image depth. Vascularization of the left kidney was subjectively assessed based on the intensity of vascular signals of the cortex and medulla by applying a scale of 1 to 4: 1, normal uniform cortical flow; 2, mild peripheral cortical hypoperfusion; 3, vascular pruning in cortex and medulla; and 4, no visible parenchymal flow, with flow seen only in central vessels [5].

CEUS was performed by using the same transducer after reducing the transmitted energy to a magnitude of 7% via a mechanical index setting of 0.07 and settings of 15 Hz and 64% gain for the pulse repetition frequency. CEUS images of left kidneys were continuously stored for 120 sec after initiation of a bolus injection of contrast medium (SonoVue; Bracco Imaging, Italy), 2.5 mg per dog, into the cephalic vein via a three-way stopcock with a 20 G IV catheter, immediately followed by the rapid injection of 5 mL of 0.9% saline. The contrast medium was shaken just before each injection and contrast study was completed within 2 h after opening of the medium container. The acquired dynamic cine loops were analyzed at 15 frames/sec by using integrated software (SOP-ALPHA7-14; Hitachi-Aloka). Each circular-shaped region of interest (5 mm diameter) was placed over the renal cortex and medulla at the same depth in order to avoid the arcuate, interlobar, and interlobular arteries and veins (Fig. 2). After a time-intensity curve was drawn of each region of interest, peak intensity, time to peak intensity, and AUC were determined.

For the induction of renal IRI, the dogs, after a 12 h fast, were

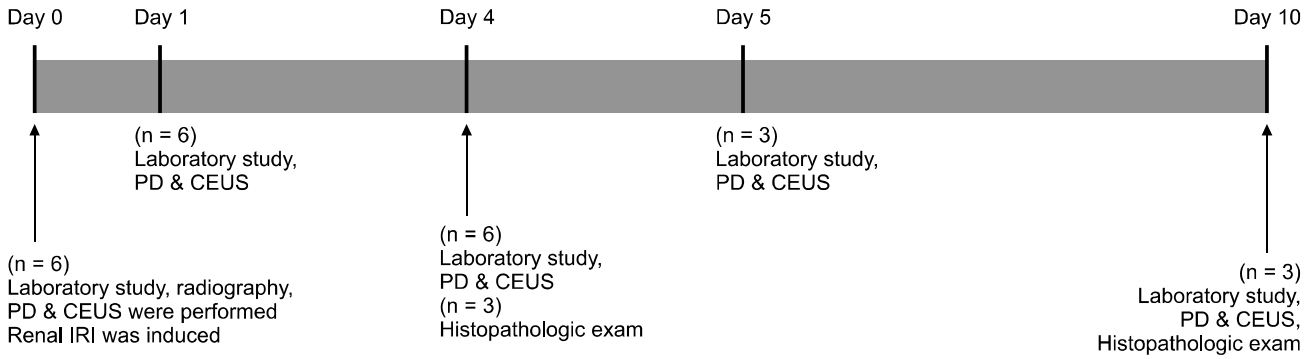

Fig. 1. Schedule diagram showing timing of laboratory examination, power Doppler (PD) and contrast-enhanced ultrasonography (CEUS), and histopathologic examination. Laboratory study included assessment of blood pressure, serum blood urea nitrogen and creatinine, urine-specific gravity and urinary protein to creatinine ratio. The number of animals used at each day is shown.

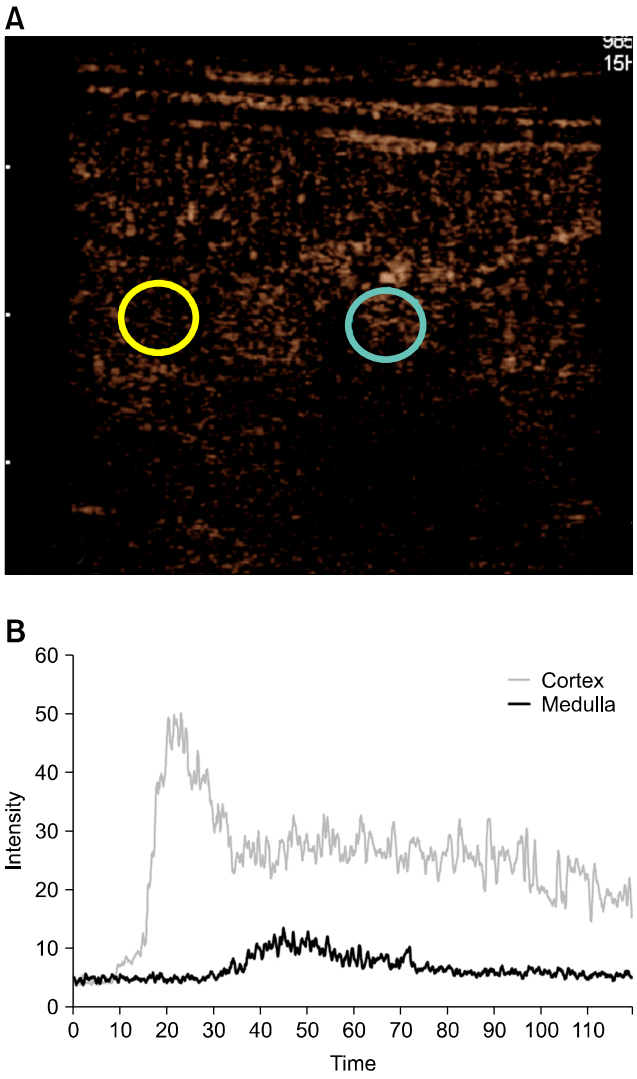

Fig. 2. Two regions of interest were placed over the renal cortex (yellow circle) and medulla (blue circle) (A), and time-intensity curves were created (B). After contrast-enhanced ultrasonography contrast agent introduction, the renal cortex showed a rapid, homogeneous, and intense enhancement pattern, while the medulla was enhanced more gradually and with a heterogeneous pattern.

first anesthetized with a combination of zolazepam/tiletamine and medetomidine by intramuscular injection with isoflurane (Rhodia Organique Fine, UK) maintenance. After a midline incision was created, the left renal artery and vein were exposed and clamped with a bulldog clamp (Kasco, Pakistan) for 60 min and then unclamped [15,19]. Because a single kidney model was adopted in this study, the right kidney was removed to eliminate the possibility that a normal right kidney would moderate actual renal functional losses of the left kidney. Tramadol hydrochloric acid (Tramadol; DongKwang Pharm, Korea) 3 mg/kg and cefazolin sodium (Cefozol; Hankook Korus Pharm, Korea) 20 mg/kg were administered before surgery and daily for 5 days after surgery. Euthanasia for kidney sampling was performed in three dogs at days 4 and 10. A balanced electrolyte solution at a rate of 10 mL/kg/h was infused during surgery and for 8 h postoperatively. The dogs were kept in cages individually and fed commercial dry food and water *ad libitum*.

Based on the results of previous studies showing that renal damage increased until day 4–5 after renal IRI and then recovered [1], blood pressure, serum BUN and creatinine, urine-specific gravity and UPC were measured at days 1, 4, 5, and 10 and conventional ultrasonography, power Doppler, and CEUS were performed at days 1, 5, and 10.

Three of six dogs were randomly selected and euthanized on day 4, while the remaining dogs were sacrificed on day 10 for histological examination and immunohistochemical assessment. Renal samples were sectioned at 3 μm along the cortex to the medulla of the kidney and at least three sections were examined by two pathologists (KO Cho and JG Park in this study). Each specimen was stained with hematoxylin and eosin and periodic acid-Schiff, and tubular epithelial cell necrosis was graded [11] as: 0, no identifiable injury; 1, necrosis of individual tubular cells; 2, necrosis of all cells in adjacent proximal convoluted tubules with survival of surrounding tubules; 3, necrosis confined to the distal third of the proximal convoluted tubules with a band of necrosis extending across the inner cortex; and 4, necrosis affecting all three segments of the proximal convoluted tubule. Terminal deoxynucleotidyl transferase–mediated dUTP nick-end labeling (TUNEL) was used to detect apoptosis by using the *In Situ* Cell Death Detection Kit, POD (Roche, Germany). Negative control sections were obtained by substituting the label solution for the TUNEL reaction mixture. To calculate the number of apoptosis-positive cells in the kidney tissues, 10 fields per section were examined by using a 40× objective and a 10× eyepiece, yielding a final magnification of 400×. The apoptotic index was established as the percentage of TUNEL-positive cells relative to the number of tubular epithelial cells. The degree of apoptosis in epithelial cells of the proximal convoluted, loop of Henle, distal convoluted, and collecting tubules was scored on a scale of 0 to 4: 0, 0%; 1, minimal (0–5%); 2, mild (5–25%); 3, moderate (25–75%); and 4, severe (75–100%).

All clinical and ultrasonographic data are presented as median and interquartile range values. Differences in peak intensity, time to peak intensity, and AUC between days were evaluated by using repeated-measures analysis of variance. The Wilcoxon signed rank test was used to compare the CEUS perfusion parameters before and after examination. P values $<$ 0.05 were considered statistically significant. Histopathological apoptosis and necrosis scores among the examined days were analyzed by two-way analysis of variance. All histopathological scores are expressed as median and interquartile range values, and p values $<$ 0.001 were considered statistically significant.

The correlation between the quantitative CEUS parameters and the histopathological scores for determining renal damage each day were analyzed by conducting Spearman rank correlation analysis. Statistical analyses were performed by using SPSS Statistics 21 (IBM, USA).

Results

After IRI induction, mean blood pressure, serum BUN and creatinine, and UPC were elevated and urine-specific gravity reduced at day 1 compared to those at baseline (Table 1). Maximum increases in serum BUN and creatinine, along with moderate to severe systemic hypertension, hyposthenuria, and severe proteinuria developed on day 4. At day 10, all parameters returned to the reference range, with the exception of for BUN and creatinine concentrations that remained above the reference range. A hyperechoic change in the renal cortex was ultrasonographically observed on day 1 and was maintained without increasing or decreasing during the 10-day observation period in all dogs. On power Doppler ultrasonography, the uniform cortical flow (score = 1) at baseline changed at day 1 after IRI induction with decreasing vascularization observed in only a few interlobar and arcuate vessels (median score, 2.5; interquartile range, 1 to 3). Vascularization was minimized, showing only peripheral cortical hypoperfusion with vascular pruning, at day 5 (median score, 3; interquartile range, 3) and then improved at day 10 (median score, 2; interquartile range, 2).

Prior to IRI induction, the contrast signal shifted rapidly from the renal sinus to the renal capsule within 3 to 6 sec after injection of the contrast agent on CEUS. Subsequently, the renal cortex was rapidly enhanced, both homogeneously and intensely (Fig. 3). Contrast enhancement of the cortex then plateaued or mildly progressed to a peak, during which time the medulla began to be contrast-enhanced more gradually and heterogeneously. Contrast enhancement of the medulla was subjectively slower and more mildly hypoechoic than that in the cortex throughout the contrast agent inflow and outflow periods. After IRI induction, enhancement of the renal cortex was delayed, and the intensity apparently reduced along with prolonged contrast agent extinction. The enhancement within

Table 1. Laboratory parameters during induced renal ischemia-reperfusion injury

Parameter	Baseline (n = 6)	Day 1 (n = 6)	Day 4 (n = 6)	Day 5 (n = 3)	Day 10 (n = 3)
BP (mmHg)	133.65 (131.58–135.73)	170.00 (148.75–187.50)	172.50 (161.25–185.25)	172.00 (162.50–193.50)	138.00 (126.50–145.00)
BUN (mg/dL)	18.50 (18.00–20.50)	63.50 (42.75–91.00)	12.00 (78.75–162.00)	111.00 (89.75–172.00)	12.00 (76.50–170.00)
Creatinine (mg/dL)	0.70 (0.70–0.78)	2.85 (2.03–4.28)	4.00 (2.80–5.50)	5.85 (4.48–7.00)	1.30 (1.2–5.9)
USG	1.05 (1.03–1.06)	1.02 (1.01–1.04)	1.02 (1.01–1.02)	1.01 (1.01–1.02)	1.02 (1.01–1.03)
UPC	0.19 (0.17–0.21)	0.45 (0.32–0.58)	3.34 (2.00–3.45)	0.46 (0.31–0.62)	0.19 (0.13–0.32)

Data are presented as median (interquartile range) values. BP, blood pressure; BUN, blood urea nitrogen; USG, urine-specific gravity; UPC, urinary protein to creatinine ratio.

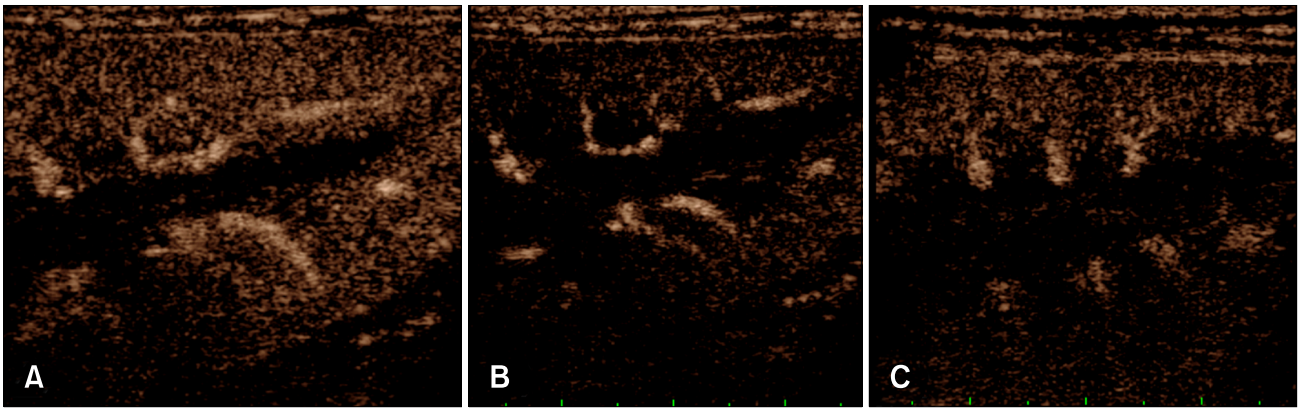

Fig. 3. Contrast-enhanced ultrasonography images obtained at the time of peak intensity in the renal cortex at baseline (A), day 4 (B), and day 10 (C). At baseline, the renal cortex showed a homogeneous and intense enhancement pattern. At day 4, the renal cortex showed noticeably reduced contrast enhancement intensity. At day 10, there was increased intensity compared to that at day 4.

the medulla showed a heterogeneous pattern that was first observed at the periphery and then gradually seen within the inner portions.

Peak intensity and AUC of the renal cortex showed similar patterns during the progression of renal damage. Both parameters began to decrease on day 1, about 20% lower than the baseline, and reached their lowest levels on day 4, approximately 50% of the baseline level. Peak intensity gradually increased until day 10 with the mean value increasing to 87% of the baseline level, not completely returning to baseline. AUC also gradually increased in this period, reaching a mean value of 95% of the baseline level. Peak intensity and AUC of the renal cortex on days 4 and 10 were significantly lower than the baseline values ($p < 0.05$) (Table 2). Although time to peak intensity decreased at day 1, compared to the baseline, there was no specific increasing or decreasing pattern over time. None of the three quantitative parameters measured from the renal medulla showed significant changes on any day.

Macroscopic examination of the kidney revealed multiple regions with severe linear paleness in the renal cortex and distinct congestion of medulla on day 4 and moderate diffuse paleness in the renal cortex on day 10. The epithelial cells within the proximal convoluted tubule underwent necrosis characterized by the absence of a nucleus or intracellular mineralization with detached cells, necrotic cell debris, and protein-rich fluids at day 4 on hematoxylin and eosin staining (Fig. 4). On day 10, the epithelial cells within the proximal convoluted tubule were regenerated, showing attenuation of swollen cuboidal cells with dense nuclei. However, necrotic cells lacking nuclei or with pyknosis were present, while the distal convoluted tubules contained protein-rich materials. On TUNEL assay, apoptotic cells were detected in the distal or collecting tubules rather than within the proximal tubules on day 4 and in the proximal and distal tubules on day 10. The mean tubular cell necrosis score at day 4 (3.07 ± 0.96) was much higher than that at day 10 (1.89 ± 0.90). The mean score of the TUNEL-positive cells was higher at day 10 (1.90 ± 1.31) than at day 4 (1.19 ± 1.07).

The changes in renal perfusion measured by using peak intensity and AUC values on CEUS and the necrosis scores obtained via histopathological examination showed strong correlations on day 4 (Table 3). Peak intensity had a weak correlation with necrosis and apoptosis scores on day 10. There was no correlation between power Doppler and histopathologic examination scores.

Discussion

In the present study, we showed that perfusion changes in acute renal IRI can be quantitatively evaluated by using CEUS. In addition, we examined the correlation between blood volume of the renal cortex, represented by peak intensity and AUC, and

Table 2. Quantitative indices from contrast-enhanced ultrasonography during induced renal ischemia-reperfusion injury

Region	parameter	Baseline (n = 6)	Day 1 (n = 6)	Day 4 (n = 6)	Day 5 (n = 3)	Day 10 (n = 3)
Cortex	PI	50.0 (47.5–54.5)	42.1 (38.6–44.7)	25.0 (23.8–26.5)	28.6 (27.3–30.0)	45.2 (43.6–45.6)
	TP	26999.0 (25449.0–27699.3)	19999.5 (18416.3–22782.8)	22632.5 (18765.8–23849.5)	23632.5 (21816.3–25899.5)	19399.0 (17966.0–21866.0)
	AUC	2595.4 (2537.6–2772.5)	2087.5 (1746.0–2127.9)	1243.2 (1185.2–1253.4)	1624.7 (1540.8–1912.8)	2343.2 (2314.7–2583.9)
Medulla	PI	22.3 (18.5–27.5)	34.2 (26.7–40.7)	30.2 (26.2–33.7)	34.5 (29.3–37.2)	42.0 (42.0–45.1)
	TP	43899.5 (42115.8–51183.0)	33999.5 (31615.8–35332.5)	31832.5 (30149.0–38466.0)	39033.0 (33582.5–42883.0)	38333.0 (37199.5–39899.5)
	AUC	1229.6 (940.8–1566.9)	1755.7 (1460.8–1826.6)	1469.0 (1402.0–1562.1)	1890.4 (1795.7–2052.7)	2080.4 (1888.8–2299.6)

Data are presented as median (interquartile range). PI, peak intensity; TP, time to peak intensity; AUC, area under the curve.

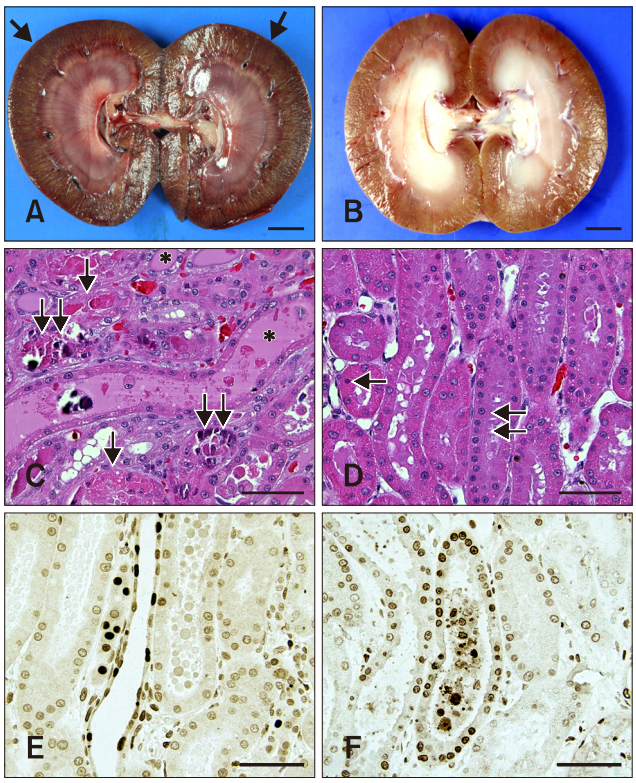

Fig. 4. Gross, histopathologic observations and TUNEL assays in the 4 and 10 days after ischemia-reperfusion injury to the kidneys. (A) Severe multiple linear paleness features (arrows) in the cortex of kidney sampled at 4 days after ischemia-reperfusion injury. Note the congestion of the medulla. (B) Moderate diffuse paleness in the cortex of the kidney sampled at 10 days after ischemia-reperfusion injury. (C) Representative histopathological lesions in the cortex of kidney sampled at 4 days after ischemia-reperfusion injury. Proximal convoluted tubular epithelial cells underwent necrosis characterized by the absence of nucleus (arrow) or intracellular mineralization (double arrow). Proximal and distal convoluted tubules contained detached cells, necrotic cell debris, and protein-rich fluids (asterisk). (D) Representative histopathological lesions in the cortex of kidney sampled at 10 days after ischemia-reperfusion injury. The epithelial cells in the proximal convoluted tubule were regenerated, showing attenuation of the swollen cuboidal cells with dense nuclei (double arrow). Necrotic cells lacking nuclei or with pyknosis (arrow) were present. The distal convoluted tubules contained protein-rich materials. (E) Cortex of kidney sampled at 4 days after ischemia-reperfusion injury. Apoptotic cells were detected in the distal or collecting tubules rather than in epithelial cells in the proximal tubules, which usually underwent necrosis. (F) Cortex of the kidney sampled at 10 days after ischemia-reperfusion injury. Apoptotic cells were detected in the proximal and distal tubules. H&E stain (C and D), terminal deoxynucleotidyl transferase–mediated dUTP nick-end labeling (E and F). Scale bars = 1 cm (A and B), 50 μm (C–F).

the degree of damage to tubular epithelial cells, determined by histopathological examination.

Canine IRI was performed by clamping the renal artery and vein for 60 min. At day 4 following IRI induction, laboratory results showed increased blood pressure, BUN, creatinine, and UPC levels and decreased urine-specific gravity suggesting that acute renal damage was induced by the IRI. Improved results were obtained on day 10 after IRI induction.

Normal kidney function in this study was contrast-enhanced on CEUS in two phases and showed an early homogeneous and intense enhancement of the renal cortex followed by a more gradual and heterogeneous enhancement of the medulla. At day 1 after IRI induction, contrast intensity of the renal cortex noticeably decreased and the onset of the renal cortical enhancement and excretion of the microbubbles were delayed and the delay was maintained until day 10. These observations indicate that perfusion of the renal cortex significantly slowed with prolongation of the contrast agent's entrance into the intrarenal capillary bed.

Peak intensity and AUC of the renal cortex decreased by about 50% on day 4 after IRI induction compared to the baseline values. At that time, massive tubular necrosis was observed within the proximal and distal convoluted tubules on histopathological examination. The hemodynamic change in the renal cortex is due to renal cortical tubular epithelial cell damage. Swelling of the epithelial cells, intratubular denuded epithelium and cellular debris, and regional necrosis of the tubular cells related to severe inflammatory reactions may induce subsequent edema of the renal tubular interstitium and lead to compression of the small blood vessels, resulting in increased vascular resistance and stasis of the microvasculature [10].

Blood volume had recovered to about 90% of the baseline level at day 10 after IRI induction. At that time, histopathological examination showed regeneration of the proximal convoluted tubular epithelial cells and decreased necrosis, although apoptotic cells were still prominent, suggesting that the tubular epithelial cells were not fully recovered. Apoptosis is triggered by the same cellular damage that precipitates necrosis but involves less severe injury than that needed to induce necrosis [28]. Real-time perfusion changes observed on CEUS during the deterioration and recovery phase, particularly the peak intensity and AUC perfusion parameters, were correlated with the degree of damage of tubular epithelial cells on the histopathological evaluation of renal IRI. In contrast, there was no significant correlation between vascular score derived by using power Doppler and histopathologic change. It indicates that CEUS is a more appropriate method than power Doppler for determining the progress of renal IRI.

Thus, after IRI induction, CEUS has the capability to evaluate renal perfusion sensitively, quantitatively, and more effectively than conventional and power Doppler ultrasonography. Increased renal echogenicity on ultrasonography can be used as an indicator for renal parenchymal diseases such as acute

Table 3. Correlation between quantitative contrast-enhanced ultrasonographyparameters and histopathological scores in kidneys after induction of ischemia-reperfusion injury

	Day 4 (n = 3)		Day 10 (n = 3)	
	PI, *r* value (*p* value)	AUC, *r* value (*p* value)	PI, *r* value (*p* value)	AUC, *r* value (*p* value)
Necrosis score	−0.810 (0.001)	−0.886 (0.001)	−0.677 (0.016)	−0.316 (0.317)
Apoptosis score	−0.396 (0.203)	−0.853 (0.139)	−0.660 (0.020)	−0.193 (0.549)

PI, peak intensity; AUC, area under the curve.

glomerulonephritis, pyelonephritis, and acute tubular necrosis [13]. However, cortical echogenicity did not increase consistent with renal parenchymal damage degree in this IRI model. Histogram analysis, an ultrasonographic function used for quantification of echogenicity, has been used to supplement gross visualization. However, various factors such as the angle and contact of the probe with the dog, pressure applied by the operator, intra-abdominal pressure of the dog, power output, gain setting, frequency, and time-gain compensation can affect histogram analysis [25]. Thus, comparison of histogram data with that of an adjacent organ such as the liver or spleen has been used to compensate for the low reproducibility of histogram results. In this study, histogram analysis was not applied to assess the cortical echogenicity; however, considering the change in cortical echogenicity seen on gross visualization, histogram analysis may have been helpful.

Vascularization of the cortex and medulla on power Doppler ultrasonography decreased immediately after IRI induction and was further deteriorated at day 5 after IRI induction, recovering on day 10. Power Doppler ultrasonography can subjectively evaluate large arteries but not cortical parenchymal perfusion [3,30]. Considering that 90% of the blood supplying the kidney enters the cortex parenchyma through the renal arterioles and capillaries, blood flow changes within the renal parenchyma instead of in the large vessels should be evaluated when estimating renal function. Moreover, microvascular tissue perfusion is a critical factor for evaluation of renal allograft dysfunction because renal vascular rejection is one of the major causes of failure after renal transplantation failure [30]. CEUS can qualitatively and quantitatively assess renal blood flow and perfusion in renal arterioles and capillaries. A recent study in human medicine reported that CEUS can identify renal arterial stenosis and thrombosis, infarction, and subtle microvascular disturbances in allograft perfusion [30].

This study has a limitation because CEUS was performed in dogs under anesthesia, which can induce hemodynamic change in kidney. Pharmacological effects of the anesthetics are mainly vasodilative, and time to peak intensity in anesthetized dogs can be faster than that measured in dogs without anesthesia. However, as estimated by histopathologic examination, blood volume rather than velocity was related with the ischemic damage in this study; thus anesthesia is not considered to have affected the study result significantly.

The present study illustrated that a change in blood perfusion can be determined by using CEUS in real time. In addition, through quantitative analysis, it was determined that CEUS-identified perfusion deterioration was correlated with renal tubular necrosis and inflammation and renal dysfunction. Although the glomerular filtration rate was not measured in the present study, renal function could be estimated based on serum BUN and creatinine levels, urine-specific gravity, and UPC. Our findings suggest that CEUS can be used as a noninvasive, quantitative diagnostic method for detecting renal IRI. However, the results of this preliminary study should be confirmed in a larger population animal study and in human clinical study. CEUS may have an important role in determining graft microvascularization in the early renal transplantation period when used as a complement to biopsy for renal graft dysfunction and as part of a therapeutic strategy for improving long-term graft survival.

Acknowledgments

This research was supported by the Basic Science Research Program through the National Research Foundation of Korea (NRF) funded by the Ministry of Science, ICT and Future Planning (2015R1A2A2A01003313), Republic of Korea.

Conflict of Interest

The authors declare no conflicts of interest.

References

1. **Adachi T, Sugiyama N, Yagita H, Yokoyama, T.** Renal atrophy after ischemia-reperfusion injury depends on massive tubular apoptosis induced by TNFα in the later phase. Med Mol Morphol 2014, **47**, 213-223.
2. **Aronson S, Thistlethwaite RJ, Walker R, Feinstein SB, Roizen MF.** Safety and feasibility of renal blood flow determination during kidney transplant surgery with perfusion

ultrasonography. Anesth Analg 1995, **80**, 353-359.
3. **Bonegio R, Lieberthal W.** Role of apoptosis in the pathogenesis of acute renal failure. Curr Opin Nephrol Hypertens 2002, **11**, 301-308.
4. **Brown ED, Chen MYM, Wolfman NT, Ott DJ, Watson NE Jr.** Complications of renal transplantation: evaluation with US and radionuclide imaging. Radiographics 2000, **20**, 607-622.
5. **Chow L, Sommer FG, Huang J, Li KC.** Power Doppler imaging and resistance index measurement in the evaluation of acute renal transplant rejection. J Clin Ultrasound 2001, **29**, 483-490.
6. **Christensson A.** Renovascular disease and renal insufficiency — diagnosis and treatment. Scand J Urol Nephrol 1999, **33**, 400-405.
7. **Chung YE, Kim KW.** Contrast-enhanced ultrasonography: advance and current status in abdominal imaging. Ultrasonography 2015, **34**, 3-18.
8. **El Morsy EM, Ahmed MAE, Ahmed AAE.** Attenuation of renal ischemia/reperfusion injury by açaí extract preconditioning in a rat model. Life Sci 2015, **123**, 35-42.
9. **Forsberg F, Basude R, Liu JB, Alessandro J, Shi WT, Rawool NM, Goldberg BB, Wheatley MA.** Effect of filling gases on the backscatter from contrast microbubbles: theory and *in vivo* measurements. Ultrasound Med Biol 1999, **25**, 1203-1211.
10. **Heffron T, Gadowski G, Buckingham F, Salciunas P, Thistlethwaite JR Jr, Stuart FP.** Laser Doppler blood flow measurement as a predictor of viability of renal allografts. Curr Surg 1990. **47**, 431-432.
11. **Ishii Y, Sawada T, Kubota K, Fuchinoue S, Teraoka S, Shimizu A.** Injury and progressive loss of peritubular capillaries in the development of chronic allograft nephropathy. Kidney Int 2005. **67**, 321-332.
12. **Jablonski P, Howden BO, Rae DA, Birrell CS, Marshall VC, Tange J.** An experimental model for assessment of renal recovery from warm ischemia. Transplantation 1983, **35**, 198-204.
13. **Jimenez C, Lopez MO, Gonzalez E, Selgas R.** Ultrasonography in kidney transplantation: values and new developments. Transplant Rev (Orlando) 2009, **23**, 209-213.
14. **Kasap B, Soylu A, Türkmen M, Kavukcu S.** Relationship of increased renal cortical echogenicity with clinical and laboratory findings in pediatric renal disease. J Clin Ultrasound 2006, **34**, 339-342.
15. **Kennedy SE, Erlich JH.** Murine renal ischaemia-reperfusion injury. Nephrology (Carlton) 2008, **13**, 390-396.
16. **Kim JM, Lee JY, Jeong SM, Park CS, Kim MC.** Attenuation of renal ischemia-reperfusion (I/R) injury by ascorbic acid in the canine nephrotomy. J Vet Clin 2010, **27**, 553-558.
17. **Ko GJ, Grigoryev DN, Linfert D, Jang HR, Watkins T, Cheadle C, Racusen L, Rabb H.** Transcriptional analysis of kidneys during repair from AKI reveals possible roles for NGAL and KIM-1 as biomarkers of AKI-to-CKD transition. Am J Physiol Renal Physiol 2010, **298**, F1472-1483.
18. **Lameire N, Van Biesen W, Vanholder R.** Acute renal failure. Lancet 2005, **365**, 417-430.
19. **Lechevallier E, Dussol B, Luccioni A, Thirion X, Vacher-Copomat H, Jaber K, Brunet P, Leonetti F, Lavelle O, Coulange C, Berland Y.** Posttransplantation acute tubular necrosis: risk factors and implications for graft survival. Am J Kidney Dis 1998, **32**, 984-991.
20. **Lee JI, Son HY, Jeong SM, Kim MC.** Amelioration effects of irrigation-aspiration on renal ischemia-reperfusion injury in canine model. J Vet Clin 2008, **25**, 257-262.
21. **Lieberthal W, Levine JS.** Mechanisms of apoptosis and its potential role in renal tubular epithelial cell injury. Am J Physiol 1996, **271**, 477-488.
22. **Lindner JR, Song J, Jayaweera AR, Sklenar J, Kaul S.** Microvascular rheology of Definity microbubbles after intra-arterial and intravenous administration. J Am Soc Echocardiogr 2002, **15**, 396-403.
23. **Liu AS, Xie JX.** Functional evaluation of normothermic ischemia and reperfusion injury in dog kidney by combining MR diffusion-weighted imaging and Gd-DTPA enhanced first-pass perfusion. J Magn Reson Imaging 2003, **17**, 683-693.
24. **Nguan CYC, Guan Q, Gleave ME, Du C.** Promotion of cell proliferation by clusterin in the renal tissue repair phase after ischemia-reperfusion injury. Am J Physiol Renal Physiol 2014, **306**, F724-733.
25. **Osawa H, Mori Y.** Sonographic diagnosis of fatty liver using a histogram technique that compares liver and renal cortical echo amplitudes. J Clin Ultrasound 1996, **24**, 25-29.
26. **Park SB, Kim JK, Cho KS.** Complications of renal transplantation: ultrasonographic evaluation. J Ultrasound Med 2007, **26**, 615-633.
27. **Schwenger V, Korosoglou G, Hinkel UP, Morath C, Hansen A, Sommerer C, Dikow R, Hardt S, Schmidt J, Kücherer H, Katus HA, Zeier M.** Real-time contrast-enhanced sonography of renal transplant recipients predicts chronic allograft nephropathy. Am J Transplant 2006, **6**, 609-615.
28. **Shuvy M, Nyska A, Beeri R, Abedat S, Gal-Moscovici A, Rajamannan NM, Lotan C.** Histopathology and apoptosis in an animal model of reversible renal injury. Exp Toxicol Pathol 2011, **63**, 303-306.
29. **Szolar DH, Preidler K, Ebner F, Kammerhuber F, Horn S, Ratschek M, Ranner G, Petritsch P, Horina JH.** Functional magnetic resonance imaging of human renal allografts during the post-transplant period: preliminary observations. Magn Reson Imaging 1997, **15**, 727-735.
30. **Trillaud H, Merville P, Tran Le Linh P, Palussière J, Potaux L, Grenier NP.** Color Doppler sonography in early renal transplantation follow-up: resistive index measurements versus power Doppler sonography. AJR Am J Roentgenol 1998, **171**, 1611-1615.
31. **Zeisbrich M, Kihm LP, Drüschler F, Zeier M, Schwenger V.** When is contrast-enhanced sonography preferable over conventional ultrasound combined with Doppler imaging in renal transplantation? Clin Kidney J 2015, **8**, 606-614.